

Cite this: *Catal. Sci. Technol.*, 2023,
13, 4684

Dinuclear chromium complexes with [OSSO]-type ligands in the copolymerization of epoxides with CO₂ and phthalic anhydride†

Fatemeh Niknam,^a Alina Denk,^b Antonio Buonerba,^{iD} Bernhard Rieger,^{iD}^b
Alfonso Grassi^a and Carmine Capacchione^{iD}*^a

In this study, a new family of dinuclear chromium complexes (**1–3**) containing bis-thioether-diphenolate ligands has been introduced for the binary copolymerization of carbon dioxide and epoxides and ternary copolymerization of the latter with phthalic anhydride. Complex **1** (0.1 mol%) in combination with (bis(triphenylphosphine)iminium chloride) (PPNCl, 0.5 mol) at 45 °C and 20 bar of CO₂ showed high regioselective copolymerization to polypropylene carbonate (PPC) with conversion (up to 91%) and selectivity (up to 95%). The data presented in this work have consistently shown that complex **1** displayed higher catalytic activity in copolymerizing epoxides with CO₂ than complexes **2**, **3**, and the analogous mononuclear **4**. At the same time, complex **1** showed good catalytic properties in the terpolymerization of epoxides/CO₂/phthalic anhydride among the tested complexes **2** and **4**. In the case of cyclohexene oxide and vinylcyclohexene oxide, a selectivity of more than 99% towards polycyclohexene carbonate (PCHC) and polyvinylcyclohexene carbonate (PVCHC) with a TOF as high as 41 h⁻¹ in the poly(ester-*block*-carbonate) was observed. Notably, a conversion higher than 99% towards the polyester block was also observed for all the studied epoxides. A bimetallic intramolecular cooperative mechanism was proposed for the copolymerization of propylene oxide and CO₂ based on the first-order dependence with respect to complex **1** by the kinetic investigations.

Received 16th June 2023,
Accepted 11th July 2023

DOI: 10.1039/d3cy00832k

rsc.li/catalysis

Introduction

Polymeric materials are ubiquitous in our world because of their unique chemical and physical properties and low cost compared to other structural materials. For decades, the sole motivation for synthesizing new polymers was obtaining a more performing material for a given application. Only recently, the growing evidence that the accumulation of plastics in the environment causes severe risks for living organisms, with serious consequences also for the food chain and, therefore, human health,^{1,2} has shifted the attention of the academic and industrial communities toward the design and synthesis of polymers that have a lesser impact on ecosystems.^{3,4}

In this scenario, aliphatic polyesters^{5–8} and polycarbonates^{9–12} have attracted much attention due to the possibility of being hydrolyzed at their end of life and being built up from renewable resources starting from cyclic esters, cyclic anhydrides, and epoxides derived from biomass and using CO₂ as a building block.^{13–16} As a matter of fact, the ring-opening copolymerization (ROCOP) of the epoxides can be performed either with CO₂, giving the corresponding polycarbonates, or with cyclic anhydrides, which gives polyester chains.^{17,18}

More recently, attention has shifted to the terpolymerization of epoxides with CO₂ and cyclic anhydrides for the possibility of obtaining block copolymers with polycarbonate and polyester segments having different microstructural features and therefore offering a wider range of chemical and physical properties.^{19–21}

In this field, dinuclear metal complexes have shown, in many cases, unique features in terms of activity and selectivity compared to their mononuclear counterparts.^{22–28} In particular, the work of the Williams research group using homodinuclear²⁹ and heterodinuclear^{30,31} complexes supported by the Robson-type cyclic ligand has shown excellent behaviour in the terpolymerization of epoxides with CO₂ and cyclic anhydrides. In all cases, the key to the good

^a Dipartimento di Chimica e Biologia “Adolfo Zambelli”, Università degli Studi di Salerno, Via Giovanni Paolo II, 84084 Fisciano, SA, Italy.

E-mail: ccapacchione@unisa.it

^b WACKER-Lehrstuhl für Makromolekulare Chemie, Zentralinstitut für Katalyseforschung (CRC), Technische Universität München, Lichtenbergstraße 4, 85747 Garching, Germany

† Electronic supplementary information (ESI) available. See DOI: <https://doi.org/10.1039/d3cy00832k>



performance of these catalysts lies in the cooperativity between the two metal centres, which allows the lowering of the barriers of the coordination/insertion steps during the copolymerization process.

[OSSO]-type metal complexes have been widely used as catalysts in many polymerization reactions,³² and more tightly Fe(III)^{33–39} and Cr(III)^{40–42} complexes have a high potential for the copolymerization of various epoxides with CO₂. Recently, we have also developed a Fe(III) dinuclear complex exhibiting good PO/CO₂ coupling performances, with kinetic data showing the cooperativity of both metal centers in the catalytic process.⁴³

Here we report on the synthesis of three new dinuclear Cr(III) complexes (1–3) based on the [OSSO]-type ligand framework and their behaviour in copolymerizing various epoxides with CO₂ and their terpolymerization with phthalic anhydride.

Results and discussion

The three new dinuclear [OSSO]-type chromium complexes 1–3 (Scheme 1) were synthesized in THF solution by reaction of the sodium salt of the corresponding pro-ligands with CrCl₃(THF)₃. All the complexes have been isolated in good yield (94–98%) as brownish microcrystalline solids.

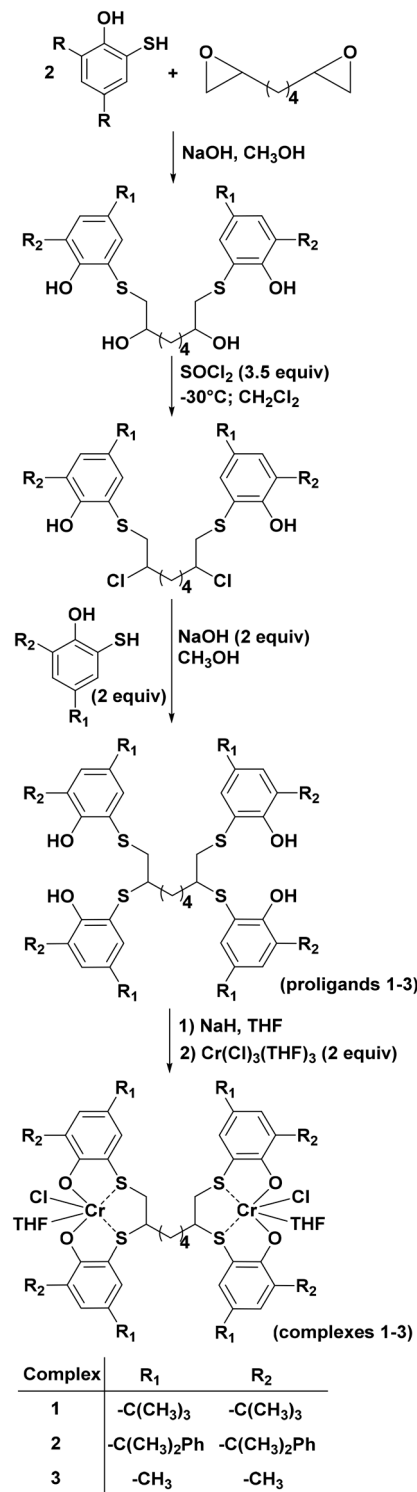
The elemental analysis of the chromium compounds was in good agreement with obtaining of the desired products. Furthermore, complexes 1–3 were also characterized by MALDI-TOF spectrometry and FT-IR (see Fig. S7–S14 of ESI†).

In addition, the Evans method, which gives indirect access to the magnetic susceptibility of paramagnetic compounds in solution, confirmed the effective magnetic moments (μ_{eff}) for 1–3 in dichloromethane-d₂ in the range between –10 and 25 °C. These values are higher than the calculated value for one isolated high spin (HS) Cr(III) centre (3.88 μ_{B}) and lower than the expected value for two isolated chromium-(III) HS nuclei (5.48 μ_{B}), suggesting an antiferromagnetic interaction between the two metal centres (see Fig. S15–S17 of ESI†), confirming the formation of dinuclear complexes stable in solution.^{42,44}

Copolymerization of epoxides with CO₂

The data relative to the copolymerization of propylene oxide with CO₂ in the presence of 1 activated by different co-catalysts, including bis(triphenylphosphine)iminium chloride (PPNCl), tetrabutylammonium bromide (TBAB), tetrabutylammonium chloride (TBAC), tetrabutylammonium azide (TBAN₃) and 4-dimethylaminopyridine (DMAP), are reported in Table 1.

Initially, we conducted experiments to find the optimized conditions for copolymerizing propylene oxide (PO) with CO₂. Concerning the co-catalysts, the combination of nucleophilicity, steric hindrance, and leaving ability play an essential role in the selectivity and activity of the catalytic system.^{45,46} As observed for the mononuclear chromium complex 4,⁴⁰ the best catalytic activity and selectivity were obtained using PPNCl in a substoichiometric amount. TBAC,



Scheme 1 Synthetic strategy of complexes 1–3.

TBAB, and DMAP are less selective in producing polypropylene carbonate, and in particular, the use of DMAP results in the exclusive formation of propylene carbonate (entry 10, Table 1).

The optimized conditions to produce polypropylene carbonate were found for catalyst loading (0.1 mol%) with 0.5



Table 1 Coupling of PO with CO₂ promoted by complex **1** and different co-catalysts

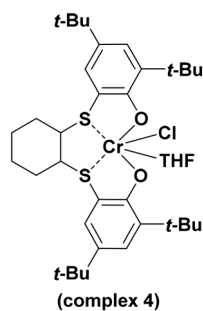
| Entry ^a | Co-cat/cat [molar ratio] | Co-cat | Conv. ^b [mol%] | PC ^{b,c} [mol%] | TOF ^d [h ⁻¹] | M _w ^e [kDa] | PDI ^e |
|--------------------|--------------------------|-------------------|---------------------------|--------------------------|-------------------------------------|-----------------------------------|------------------|
| 1 | 0.25 | PPNCl | 80 | 90 | 33 | 10.0 | 1.3 |
| 2 | 0.50 | PPNCl | 91 | 95 | 38 | 12.9 | 1.4 |
| 3 | 1.00 | PPNCl | 93 | 93 | 39 | 12.5 | 1.6 |
| 4 | 0.50 | TBAC | 67 | 46 | 28 | 6.3 | 1.3 |
| 5 | 1.00 | TBAC | 87 | 93 | 36 | 8.1 | 1.2 |
| 6 | 0.50 | TBAB | 22 | 81 | 9 | — | — |
| 7 | 1.00 | TBAB | 42 | 3 | 18 | — | — |
| 8 | 0.50 | TBAN ₃ | 71 | 89 | 30 | 17.4 | 1.4 |
| 9 | 1.00 | TBAN ₃ | 75 | 55 | 31 | 6.9 | 1.2 |
| 10 | 0.50 | DMAP | 40 | 0 | 17 | — | — |

^a Reaction conditions: PO = 0.014 mol; PO/complex **1** molar ratio = 1000; reaction time = 24 h; temperature = 45 °C; *p* CO₂ = 20 bar; co-catalyst (PPNCl (bis(triphenylphosphine)iminium chloride); TBAB = tetrabutylammonium bromide; TBAC = tetrabutylammonium chloride; TBAN₃ = tetrabutylammonium azide; DMAP = 4-dimethylaminopyridine). ^b Determined by ¹H NMR in CDCl₃. ^c Selectivity as mole percentage of polycarbonate linkage to polycarbonate + cyclic carbonate units. ^d TOF = (mol_{epoxide reacted})/(mol_{cat} × time). ^e Determined by gel permeation chromatography (GPC) with respect to polystyrene standards.

mol of PPNCl at reaction temperature (45 °C) at 20 bar of CO₂, reaching high conversion (up to 91%) and selectivity (up to 95%) to PPC with a TOF up to 38 h⁻¹ (entry 2, Table 1). For comparison, mono- and dinuclear salphen-type chromium complexes TOFs were found to be 61 h⁻¹ and 49 h⁻¹, respectively toward formation of PPC under higher catalyst loading and CO₂ pressure.²⁶ As expected, higher temperature and lower catalyst loading resulted in the production of predominantly propylene carbonate (see Table S1 of ESI†).

With the optimized conditions in hand (0.1 mol% of complex, 0.5 mol of PPNCl, 45 °C, and 20 bar of CO₂), we decided to compare, under the same reaction conditions, the catalytic activity of the complexes **1–3** and the mononuclear complex **4** (Scheme 2).

The results are summarised in Table 2. Cyclohexene oxide (CHO) and vinylcyclohexene oxide (VCHO) activated by **1** both showed complete selectivity for the polycarbonate and higher activity, reaching a TOF of 40 h⁻¹ in the case of VCHO at 80 °C (entry 9, Table 2). 1-Hexene oxide (HO) was also converted to the corresponding polycarbonate with good activity and selectivity, notably showing a higher molecular weight among the obtained polycarbonates (M_w = 23.4 kDa) (entry 13, Table 2).

**Scheme 2** Structure of complex **4**.

It is worth noting that complex **1** is the most active and selective in the copolymerization of all the investigated substrates (PO, CHO, VCHO, and HO) with the maximum molecular weight among all the other copolymerization products obtained in the presence of complexes **2** and **3** (entries 1, 5, 9, and 13, Table 2). The more sterically congested complex **2** was less active and selective (entries 2, 6, 10, 14, Table 2), and complex **3**, bearing the less bulky methyl substituents, was less chemo-selective, giving a mixture of PPC and cyclic propylene carbonate (entry 3, Table 2) and the exclusive formation of the cyclic product in the case of HO (entry 15, Table 2).

A comparison with the mononuclear complex **4** also revealed that complex **1** is significantly more active and selective toward polycarbonates in the copolymerization of PO and CHO with CO₂ (see entries 1, 4, 5, and 8 in Table 2). It is worth noting that only complexes **1** and **4** containing *tert*-butyl groups showed selectivity toward poly(1-hexene carbonate) (PHC), in which complex **1** showed again higher activity (see entries 13 and 16 of Table 2).

The two-dimensional ¹³C{¹H} NMR spectrum was recorded to provide better insight into the purified resulting copolymer microstructural features (see Fig. S19–S23 of ESI†), the only peak at δ = 154.3 ppm attributed to the carbonyl group in the case of PPC revealed a high regioselective copolymerization in which the nucleophile attacks the sterically less hindered carbon atom to open the epoxide ring, resulting in head-to-tail (HT) arrangements without regioerrors.⁴⁷ In the case of poly(cyclohexene) carbonate (PCHC) and poly(vinylcyclohexene) carbonate (PVCHC), the ¹³C{¹H}NMR analysis is in agreement with the formation of stereoirregular polymer chains (see Fig. S22 of ESI†).⁴⁸

Terpolymerization of epoxides/phthalic anhydride with CO₂

The good performances obtained in the copolymerization of the tested epoxides towards the formation of polycarbonates prompted us to investigate the terpolymerization of epoxide/



Table 2 Coupling of epoxides with CO₂ promoted by complexes 1–4

| Entry ^a | Cat | Epoxide | T [°C] | Conv. ^b [mol%] | PC ^{b,c} [mol%] | TOF ^d [h ⁻¹] | M _w ^e [kDa] | PDI ^e |
|--------------------|-----|---------|--------|---------------------------|--------------------------|-------------------------------------|-----------------------------------|------------------|
| 1 | 1 | PO | 45 | 91 | 95 | 38 | 12.9 | 1.4 |
| 2 | 2 | PO | 45 | 37 | 90 | 15 | 7.3 | 1.2 |
| 3 | 3 | PO | 45 | 20 | 54 | 23 | — | — |
| 4 | 4 | PO | 45 | 44 | 88 | 18 | 10.7 | 1.5 |
| 5 | 1 | CHO | 80 | 89 | >99 | 37 | 10.1 | 1.2 |
| 6 | 2 | CHO | 80 | 83 | >99 | 34 | 7.4 | 1.2 |
| 7 | 3 | CHO | 80 | 40 | >99 | 17 | 5.3 | 1.3 |
| 8 | 4 | CHO | 80 | 63 | >99 | 26 | 6.1 | 1.6 |
| 9 | 1 | VCHO | 80 | 97 | >99 | 40 | 14.2 | 1.4 |
| 10 | 2 | VCHO | 80 | 85 | >99 | 35 | 11.8 | 1.4 |
| 11 | 3 | VCHO | 80 | 76 | >99 | 32 | 7.1 | 1.5 |
| 12 ^f | 4 | VCHO | 80 | 94 | >99 | 39 | 13.8 | 1.9 |
| 13 | 1 | HO | 45 | 79 | 74 | 33 | 23.4 | 1.3 |
| 14 | 2 | HO | 45 | 45 | 0 | 19 | — | — |
| 15 | 3 | HO | 45 | 5 | 0 | 2 | — | — |
| 16 | 4 | HO | 45 | 33 | 80 | 14 | 16.8 | 1.3 |

^a Reaction conditions: epoxide = 0.014 mol; epoxide/complex molar ratio = 1000; reaction time = 24 h; *p* CO₂ = 20 bar; PPnCl/complex molar ratio = 0.5. ^b Determined by ¹H NMR in CDCl₃. ^c Selectivity as mole percentage of polycarbonate linkage to polycarbonate + cyclic carbonate units. ^d TOF = (mol_{epoxide reacted})/(mol_{cat} × time). ^e Determined by GPC with respect to polystyrene standards. ^f PPnCl/complex 4 molar ratio = 1.0.

CO₂/phthalic anhydride (PA) (Table 3). Complexes 1, 2, and 4 were examined under optimized conditions (0.1 mol% of complex, 0.5 mol of PPnCl, epoxide:PA = 10:1, mol/mol, and 20 bar of CO₂). The data are shown in Table 3. The reported conversions were calculated by comparing the intensity of the ¹H signals of the reagents (PO, CHO, VCHO, and HO) with those of the methine protons of polycarbonates (at δ = 4.98 ppm for PPC, δ = 4.60 ppm for PCHC, δ = 4.77 ppm for PVCHC, and δ = 4.89 ppm for PHC) and of the cyclic propylene carbonate (δ = 4.99–4.82 ppm). From the data in Table 3, complex 1 showed the highest activity in the epoxide/CO₂/PA terpolymerization. Notably, for all the studied epoxides, a conversion higher than

99% towards the polyester block was observed due to the absence of signals belonging to unreacted PA in the ¹H NMR spectrum of the resulting crude product.

The ¹H and ¹³C{¹H} NMR spectra do not show polycarbonate sequences in the polyester segments suggesting the formation of diblock poly(ester-*block*-carbonate) copolymers through the faster reaction of epoxide/anhydride coupling and, after the complete conversion of the anhydride, the carbonate block was grown by CO₂/epoxide alternating insertion.^{49,50}

Data from Table 3 can be compared with the data in Table 2, which show sensibly lower conversion in

Table 3 Terpolymerization of epoxide/CO₂/PA promoted by complexes 1, 2, and 4

| Entry ^a | Cat | Epoxide | T [°C] | Conv. ^{b,c} [mol] | PC ^{b,d} [mol%] | TOF ^e [h ⁻¹] | M _w ^f [kDa] | PDI ^f |
|--------------------|-----|---------|--------|----------------------------|--------------------------|-------------------------------------|-----------------------------------|------------------|
| 1 | 1 | PO | 45 | 62 | 88 | 29 | 12.3 | 1.2 |
| 2 | 2 | PO | 45 | 55 | 94 | 25 | 13.0 | 1.6 |
| 3 | 4 | PO | 45 | 60 | 88 | 29 | 19.0 | 1.4 |
| 4 | 1 | CHO | 80 | >99 | >99 | 41 | 11.0 | 1.3 |
| 5 | 2 | CHO | 80 | 77 | >99 | 32 | 9.6 | 1.2 |
| 6 | 4 | CHO | 80 | 81 | >99 | 34 | 10.5 | 1.2 |
| 7 | 1 | VCHO | 80 | >99 | >99 | 41 | 12.0 | 1.3 |
| 8 | 2 | VCHO | 80 | 89 | >99 | 37 | 12.7 | 1.4 |
| 9 | 4 | VCHO | 80 | 77 | >99 | 32 | 11.6 | 1.3 |
| 10 | 1 | HO | 45 | 67 | 93 | 30 | 8.5 | 1.0 |
| 11 | 2 | HO | 45 | 0 | 0 | 0 | — | — |
| 12 | 4 | HO | 45 | 58 | 91 | 26 | 9.0 | 1.1 |

^a Reaction conditions: epoxide = 0.014 mol; epoxide/complex molar ratio = 1000; PPnCl/complex molar ratio = 0.5; reaction time = 24 h; epoxide:PA molar ratio = 10:1; *p* CO₂ = 20 bar; co-catalyst = PPnCl. ^b Determined by ¹H NMR in CDCl₃. ^c The ester-selectivity in the polyester segment/block >99%. ^d Selectivity as mole percentage of polycarbonate linkage to polycarbonate + cyclic carbonate units. ^e TOF = (mol_{epoxide reacted})/(mol_{cat} × time). ^f Determined by GPC with respect to polystyrene standards.



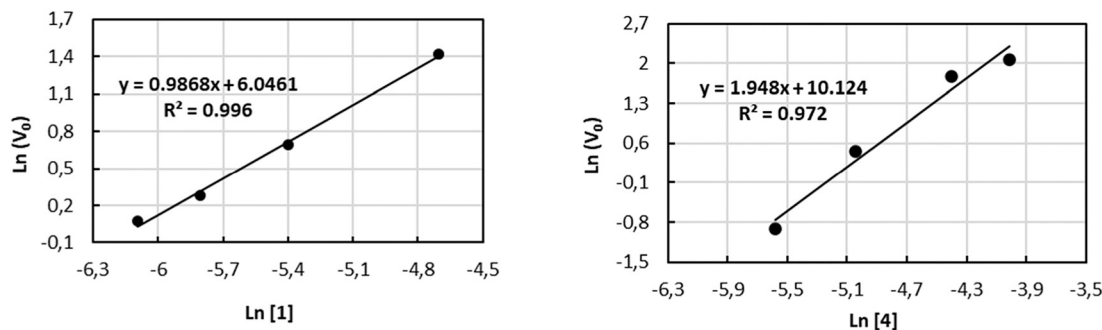


Fig. 1 Plot of $\ln(v_0)$ for the formation of PPC versus: (left) $\ln[1]$, (right) $\ln[4]$.

terpolymerization toward PPC and PHC activated by complex **1** (see entries 1 and 10, Table 3). In contrast, CHO and VCHO have been converted more than 99% (TOF of 41 h^{-1}) to their related polycarbonates (entries 4, and 7, Table 3). A negligible amount of polyether (peak at $\delta = 3.45 \text{ ppm}$ in the ^1H NMR spectrum) was observed in the terpolymerization reaction of CHO/PA with CO_2 (see Fig. S27 of ESI†). DOSY NMR spectroscopy for purified poly(ester-*block*-cyclohexene carbonate) (PE-*co*-PCHC) and poly(ester-*block*-vinylcyclohexene carbonate) (PE-*co*-PVCHC) was carried out (see Fig. S28 and S29 of ESI†). It is apparent that all signals show the same diffusion coefficient, indicating the existence of a genuine copolymer. Interestingly, in the $^{13}\text{C}\{^1\text{H}\}$ NMR spectra of terpolymers, the chemical shifts and patterns of the carbonyl groups in the backbone of polycarbonates are similar to those observed for copolymers. This finding agrees with our earlier observation for polypropylene carbonate, which shows that the PO/ CO_2 terpolymerization with PA is also regioselective (see Fig. S24–S26 of ESI†). The thermal properties of the poly(ester-*block*-carbonate)s show that the presence of a semi-aromatic polyester block due to the presence of PA in the polymer chain causes an increase in the T_g values compared to the corresponding polycarbonates. As already reported for these diblock copolymers, the phases are completely miscible; therefore, only one value for T_g was observed (see Fig. S18 of ESI†).⁵¹

Kinetic studies

The kinetic investigations for **1** and **4** with combinations of PPnCl as catalytic systems were performed for a more detailed understanding of the copolymerization process towards the formation of PPC. *In situ* attenuated total reflection infrared (ATR-IR) spectroscopy provides a valuable tool for monitoring the reaction progress by increasing the carbonyl stretching bond ($\nu_{\text{C=O}} = 1750 \text{ cm}^{-1}$) (see Fig. S39–S46 of the ESI†). The solution of PO/ CH_2Cl_2 /PPnCl was prepared as the reaction medium to guarantee the homogeneity of the system during the experiment. The reaction order with respect to **1** and **4** was determined by performing a series of experiments varying the concentration of **1** (in the range from 2.26 to 9.03 mM) and of **4** (in the range from 3.76 to 18.05 mM) while keeping the

concentration of PPnCl constant at 2.26 mM (see Tables S2 and S3 of ESI†). The values of initial velocities v_0 were obtained from the slope of the initial straight line at low conversion of the epoxide. The double logarithmic plot of the initial rate (v_0) versus the concentration of the complexes gave orders of 0.98 and 1.94, very close to first-order and second-order dependences with respect to complexes **1** and **4**, respectively (see Fig. 1).

These data support the involvement of two metal centres during the polymerization process, as already observed in other dinuclear systems,^{52,53} in which the presence of two vicinal metal centers allows coordination and ring opening of the incoming monomer (epoxide, CO_2) and the chain growth on the second metal center. The higher activity and selectivity observed for dinuclear complex **1** *vis-à-vis* complex **4** are therefore a consequence of a cooperative mechanism due to the proximity of the two metal centres.

Conclusions

This study set out to report the synthesis of a new series of dinuclear Cr(III) complexes (**1–3**), supported by bis-thioether-diphenolate ligand and their catalytic activity in combination with PPnCl as a co-catalyst to promote the reaction of epoxides with CO_2 . It was observed that the activity of complexes mainly relied on the nature of the substituents present in the phenolate group. Complex **1** with *tert*-butyl substitutions displayed good activity and selectivity for the formation of polycarbonates starting from the corresponding epoxides as compared to complexes **2**, **3**, and the analogous mononuclear **4**. In the case of PO, a high conversion (up to 91%, with a TOF up to 38 h^{-1}) to polypropylene carbonate with negligible production of the cyclic carbonate during a regioselective copolymerization was observed. **1** showed good catalytic properties in the terpolymerization of epoxide/ CO_2 /phthalic anhydride among all the other tested complexes **2** and **4**. In the case of CHO and VCHO, a selectivity of more than 99% towards PCHC and PVCHC with a TOF as high as 41 h^{-1} in the poly(ester-*block*-carbonate) was observed. The kinetic investigation supported the occurrence of the bimetallic intramolecular and bimetallic intermolecular ring-opening mechanisms by observation of the first-order and



second-order dependences with respect to the complexes **1** and **4**, respectively.

Experimental part

General considerations

All syntheses containing air- and moisture-sensitive compounds were performed under a dry nitrogen atmosphere using standard Schlenk techniques and the Jacomex glovebox. All chemicals and solvents were purchased from Sigma Aldrich or TCI. THF (99%) was refluxed for 72 hours over sodium and sodium benzophenone ketyls and distilled before use for moisture- and oxygen-sensitive reactions. Monomers were dried over calcium hydride, distilled, and stored over activated 4 Å molecular sieves prior to polymerization.

NMR (^1H , ^{13}C , Dosy, and HSQC) measurements were recorded on Bruker Avance spectrometers (300, 400, or 600 MHz). Chemical shifts δ were reported in ppm and referenced to tetramethylsilane (TMS), and calibrated to the residual ^1H or ^{13}C signal of the deuterated solvent. Deuterated solvents were obtained from Aldrich and dried over a 3 Å molecular sieve.

Measurements of effective magnetic moments (μ_{eff}) were performed on Bruker Avance spectrometers (300 and 600 MHz) in deuterated solvent (dichloromethane- d_2) using a 5 mm Wilmad coaxial insert NMR tube.³³ The effective magnetic moment (μ_{eff}) was calculated from $\mu_{\text{eff}} = 8\chi_g M_w T$. The χ_g ($\text{cm}^3 \text{g}^{-1}$) is the corrected molar susceptibility derived from $\chi_g = 3\Delta f/4\pi f_0 C M_w + \chi_o$. Δf (Hz) is the shift in frequency of the residual proton signal of the solvent in the presence of the complex from the value of the pure solvent. C (mol cm^{-1}) is concentration, M_w (g mol^{-1}) is the molecular weight of the complex, f_0 (Hz) is the operating frequency of the spectrometer, and χ_o is the mass susceptibility of the pure solvent ($-0.5486 \times 10^{-6} \text{ cm}^3 \text{g}^{-1}$ for dichloromethane- d_2). $4\pi/3$ is the shape factor for a cylindrical sample in a superconducting magnet.

DSC was conducted on a DSC Q2000 instrument. 3–10 mg of the polymer was filled into a DSC aluminum pan and heated from -80 to 170 °C at a rate of 5 K min^{-1} . The reported values were determined with TA Universal Analysis from the second heating cycle.

MALDI-TOF analysis was performed on a Waters Quattro Micro triple quadrupole mass spectrometer equipped with an electrospray ion source. Anthracene and 2,5-dihydroxybenzoic acid were used as matrixes.

GPC was performed on a Varian PL-GPC 50 equipped with a Deflection RI detector to obtain size exclusion chromatography (SEC) measurements. Polystyrene was used as a standard at 40 °C with THF (flow = 1 mL min^{-1}) as an eluent.

FT-IR measurements were carried out on a Bruker Vertex 70 spectrometer equipped with a DTGS detector and a Ge/KBr beam splitter, analyzing the solid state as KBr disks. *In situ* IR measurements for kinetic investigations were

performed under an argon atmosphere using an ATR IR Mettler Toledo system.

Synthesis

Both the ligands 6,6',6''-(pentane-1,2,4,5-tetrayltetrakis(sulfanediyl)) tetrakis(2,4-bis(2-phenylpropan-2-yl)phenol), (**L**₂), 6,6',6''-(octane-1,2,7,8-tetrayltetrakis(sulfanediyl)) tetrakis(2,4-dimethylphenol), (**L**₃), and the complexes (**1**–**3**) were synthesized according to the literature procedures.⁴¹

Synthesis and characterization of L₂. The mixture of 2-mercapto-4,6-bis(2-phenylpropan-2-yl)phenol (16.0 mmol) and NaOH (16.0 mmol) in 70 ml of methanol was refluxed until complete dissolution of all reagents. Then the mixture was cooled at 25 °C for 20 minutes. After that, 1,2,7,8-diepoxyoctane (8.0 mmol) was added, and the mixture refluxed overnight. The methanol was evaporated, and water (50 ml) was added. The organic phase was extracted by diethyl ether (3×50 ml) and dried over MgSO_4 . After evaporation of the solvent, the pro-ligand **b** was precipitated from cold petroleum ether and *n*-hexane as a white solid. Yield 80%. ^1H NMR (CDCl_3): $\delta = 7.21$ – 7.31 (m, 20H, arom. CH); 7.20 (d, 2H, Ar-H); 7.17 (br s, 2H, Ar-OH); 7.14 (d, 2H, Ar-H); 3.76 (br s, 1H, CH_2 -CH-(OH)); 3.36 (br s, 1H, CH_2 -CH-(OH)); 3.21 (m, 1H, CH_2 -CH-(OH)); 2.60 (ddd, 4H, S- CH_2); 2.02 (m, 1H, CH_2 -CH-(OH)); 1.69 (s, 12H, CH_3); 1.61 (8H, $(\text{CH}_2)_4$ -alkyl bridge); 1.56 (12H, 4 CH_3). Compound **b** (8.0 mmol) was dissolved in dichloromethane (30 ml) and stayed in a cooling bath (-30 °C) for 20 minutes. After that, thionyl chloride (28.0 mmol) was added dropwise into the solution. After getting to room temperature (10 minutes), the mixture refluxed overnight. Then the solvent was concentrated and dissolved in diethyl ether (80 ml) and washed with a solution of NaHCO_3 (10% w/w, 50 ml). The organic phase was dried with MgSO_4 , filtered, and concentrated. The pro-ligand **c** was obtained as a light-yellow oil. Yield 74%. ^1H NMR (CDCl_3): $\delta = 7.19$ – 7.34 (m, 20H, arom. CH); 7.17 (m, 4H, Ar-H); 7.15 (br s, 2H, Ar-OH); 3.70 (m, 2H, CHCl); 3.28 (m, 1H, CH_2 -alkyl bridge); 2.86 (m, 4H, S- CH_2); 2.21 (d, 1H, CH_2 -alkyl bridge); 1.70 (s, 12H, 4 CH_3); 1.65 (4H, CH_2 -alkyl bridge); 1.63 (br s, 6H, 2 CH_3); 1.56 (s, 6H, 2 CH_3); 1.51 (br s, 1H, CH_2 -alkyl bridge); 1.48 (br s, 1H, CH_2 -alkyl bridge).

The mixture of 2-mercapto-4,6-bis(2-phenylpropan-2-yl)phenol (16.0 mmol) and NaOH (16.0 mmol) in 70 ml of methanol was refluxed until complete dissolution of all reagents. After 20 minutes at 25 °C, compound **c** (8.0 mmol) was dissolved in the minimum amount of methanol and added dropwise into the mixture of solutions. The mixture was refluxed over night at 70 °C. After that, the solvent was evaporated, and 50 ml of water was added. The organic phase was extracted by diethyl ether (3×50 ml) and dried with MgSO_4 . The concentrated solution was precipitated from methanol in the fridge as a brownish solid. Yield 70%. ^1H NMR (CDCl_3): $\delta = 7.12$ – 7.27 (m, 40H, arom. CH); 7.08 (s, 8H, Ar-H); 6.62 (br s, 2H, Ar-OH); 6.42 (br s, 2H, Ar-OH); 2.50 (br s, 6H), 1.67 (m, 28H, CH_3 and $(\text{CH}_2)_2$ -alkyl bridge); 1.61 (s,



28H, CH₃ and (CH₂)₂-alkyl bridge); ¹³C{¹H} NMR (CDCl₃): δ 153.9; 153.0; 151.0; 150.8; 150.6; 142.4; 142.1; 135.1; 133.8; 132.2; 128.5; 128.4; 128.3; 127.1; 126.1; 126.0; 125.8; 125.7. Elemental analysis calcd. for C₁₀₄H₁₁₄O₄S₄ = C 80.26, H 7.38, O 4.11, S 8.24; found: C 80.46, H 7.33, O 4.16, S 8.34; MS: *m/z* = 1578.7 (L₂ + Na)⁺, 1593.7 (L₂ + K)⁺.

Synthesis and characterization of L₃. The mixture of 2-mercapto-4,6-dimethylphenol (16.0 mmol) and NaOH (16.0 mmol) in 70 ml of methanol was refluxed until complete dissolution of all reagents. Then the mixture was cooled at 25 °C for 20 minutes. After that, 1,2,7,8-diepoxyoctane (8.0 mmol) was added, and the mixture refluxed overnight. The methanol was evaporated, and water (50 ml) was added. The organic phase was extracted by diethyl ether (3 × 50 ml) and dried over MgSO₄. After evaporation of the solvent, the pro-ligand **b**, obtained as a light-yellow oil. Yield 70%. ¹H NMR (CDCl₃): δ = 7.11 (s, 2H, Ar-H); 6.93 (s, 2H, Ar-H); 6.88 (s, 2H, Ar-OH), 3.60 (br s, 2H, CH₂-CH-(OH)); 2.75 (ddd, 4H, S-CH₂); 2.23 (s, 6H, 2CH₃); 2.21 (s, 6H, 2CH₃); 2.19 (d, 2H, CH₂-alkyl bridge); 1.46 (m, 6H, CH₂-alkyl bridge). Compound **b** (8.0 mmol) was dissolved in dichloromethane (30 ml) and stayed in a cooling bath (-30 °C) for 20 minutes. After that, thionyl chloride (28.0 mmol) was added dropwise into the solution. After getting to room temperature (10 minutes), the mixture refluxed overnight. Then the solvent was concentrated and dissolved in diethyl ether (80 ml) and washed with a solution of NaHCO₃ (10% w/w, 50 ml). The organic phase was dried with MgSO₄, filtered, and concentrated. The pro-ligand **c** was obtained as a light-brown oil. Yield 74%. ¹H NMR (CDCl₃): δ = 7.11 (s, 2H, Ar-H); 6.97 (s, 2H, Ar-H); 6.62 (s, 2H, Ar-OH); 3.88 (br s, 2H, -CH₂-CH-(OH)); 3.60 (m, 2H, CH₂-alkyl bridge); 3.50 (m, 3H, CH₂-alkyl bridge); 3.00 (m, 4H, S-CH₂); 2.40 (m, 3H, CH₂-alkyl bridge); 2.24 (br s, 12H, 4CH₃).

The mixture of 2-mercapto-4,6-dimethylphenol (16.0 mmol) and NaOH (16.0 mmol) in 70 ml of methanol was refluxed until complete dissolution of all reagents. After 20 minutes at 25 °C, compound **c** (8.0 mmol) was dissolved in the minimum amount of methanol and added dropwise into the mixture of solutions. The mixture was refluxed over night at 70 °C. After that, the solvent was evaporated, and 50 ml of water was added. The organic phase was extracted by diethyl ether (3 × 50 ml) and dried with MgSO₄. The concentrated solution was washed with cold methanol and collected as a yellow, transparent oil. Yield 60%. ¹H NMR (CDCl₃): δ = 7.02 (s, 2H, Ar-H); 6.99 (s, 2H, Ar-H); 6.93 (s, 2H, Ar-H); 6.90 (s, 2H, Ar-H); 6.87 (br s, 2H, Ar-OH); 6.71 (br s, 2H, Ar-OH); 2.80 (m, 6H); 2.32 (s, 1H, CH-alkyl bridge); 2.25 (br s, 6H, 2CH₃); 2.24 (br s, 2H, (CH₂)₂-alkyl bridge); 2.22 (br s, 6H, 2CH₃); 2.19 (br s, 12H, 4CH₃); 1.69 (m, 2H, CH₂-alkyl bridge); 1.55 (m, 3H, CH₂-alkyl bridge); ¹³C{¹H} NMR (CDCl₃): δ 154.1; 153.4; 134.5; 134.1; 133.7; 133.5; 132.1; 129.8; 129.6; 124.7; 117.6; 115.7; 50.56; 41.9; 33.5; 26.9; 20.7; 16.85. Elemental analysis calcd. for C₄₀H₅₀O₄S₄ = C 66.44, H 6.97, O 8.85, S 17.74; found: C 66.54, H, 6.90, O, 8.83, S, 17.77; MS: *m/z* = 745.2 (L₃ + Na)⁺, 761.2 (L₃ + K)⁺.

Synthesis of 1. The ligand L₁ (0.50 g, 0.47 mmol) was dissolved in dried THF (30 ml). Then the solution was added to the suspension of NaH (0.05 g, 2.35 mmol) in THF (20 ml), and the mixture was stirred at room temperature overnight. After that, the yellow mixture was filtered through celite and slowly added to the solution of Cr(Cl)₃(THF)₃ (0.35 g, 0.94 mmol) in THF (30 ml). The color of the solution changed to dark brown, and the reaction was kept at 25 °C overnight. The resulting mixture was filtered through celite, and after removing the solvent under vacuum, the final product was obtained as a dark brownish solid (yield 98%). Elemental analysis calcd. for C₇₂H₁₁₀Cl₂Cr₂O₆S₄ = C 62.90, H 8.07, Cl 5.16, Cr 7.56, O 6.98, S 9.33; found: C 62.95, H 8.13, Cl 5.20, Cr 7.48, O 6.90, S 9.23; MS: *m/z* = 1412.4 (1 + K)⁺.

Synthesis of 2. The ligand L₂ (1.00 g, 0.64 mmol) was dissolved in dried THF (30 ml). Then the solution was added to the suspension of NaH (0.07 g, 3.20 mmol) in THF (20 ml), and the mixture was stirred at room temperature overnight. After that, the yellow mixture was filtered through celite and slowly added to the solution of Cr(Cl)₃(THF)₃ (0.48 g, 1.28 mmol) in THF (30 ml). The color of the solution changed to dark brown, and the reaction was kept at 25 °C overnight. The resulting mixture was filtered through celite, and after removing the solvent under vacuum, the final product was obtained as a brownish solid (yield 98%). Elemental analysis calcd. for C₁₁₂H₁₂₆Cl₂Cr₂O₆S₄ = C 71.89, H 6.79, Cl 3.79, Cr 5.56, O 5.13, S 6.85; found: C 71.93, H 6.72, Cl 3.83, Cr 5.63, O 5.03, S 6.75; MS: *m/z* = 1641.6 (2-THF-Cl)₂-(O)H⁺.

Synthesis of 3. The ligand L₃ (0.5 g, 0.69 mmol) was dissolved in dried THF (30 ml). Then the solution was added to the suspension of NaH (0.08 g, 3.45 mmol) in THF (20 ml), and the mixture was stirred at room temperature overnight. After that, the yellow mixture was filtered through celite and slowly added to the solution of Cr(Cl)₃(THF)₃ (0.52 g, 1.28 mmol) in THF (30 ml). The color of the solution changed to dark green, and the reaction was kept at 25 °C overnight. The resulting mixture was filtered through celite, and after removing the solvent under vacuum, the final product was obtained as a dark green solid (yield 98%). Elemental analysis calcd. for C₄₈H₆₂Cl₂Cr₂O₆S₄ = C, 55.53, H 6.02, Cl 6.83, Cr 10.02, O 9.25, S 12.35; found: C, 55.48, H 6.08, Cl 6.87, Cr 10.00, O 9.20, S 12.30; MS: *m/z* = 967.1 (3-THF)⁺, 949.2 (3-THF-H₂O)⁺.

Polymerization and terpolymerization

The reaction vessels, needles, and 60 mL stainless steel reactor were dried in an oven at 140 °C for 24 hours before use. Complexes 1–3, PPNCl, and/or phthalic anhydride were weighed in the glovebox. The calculated amount of epoxides was taken under nitrogen flow and added to the vial containing complex and PPNCl. Then the mixture of solutions was injected into the reactor and fed with CO₂. The catalytic reactions were run at an adjusted temperature for 24 hours. At the end of the reaction, the reactor was cooled with ice for 20 minutes, and then the CO₂ was slowly released. A



small portion of the reaction mixture was used for ^1H NMR spectroscopy for the determination of conversion and selectivity. The crude polymer products were collected by dissolving them in a minimum amount of CH_2Cl_2 and washing them with methanol. After the consequent removal of the solvent, the precipitated polymers were dissolved in dichloromethane and then dried under vacuum for 24 hours.

Kinetic investigations

The kinetic studies of polymerizations were performed with *in situ* monitoring using a React-IR Mettler-Toledo system. The 50 mL steel autoclave, equipped with a diamond window, a heating device, and mechanical stirring, was heated to 130 °C under vacuum overnight prior to polymerization. All chemicals were weighed in the glove box, stored in syringes, and rapidly transported to the reactor. The reaction was terminated when the signal of the carbonyl oxygen (1750 cm^{-1}) was constant by adding dichloromethane and some drops of methanol.

Author contributions

Fatemeh Niknam, investigation, methodology, synthesis, formal analysis, writing – original draft. Alina Denk, investigation, methodology. Antonio Buonerba, investigation, resources, writing – review & editing. Bernhard Rieger, visualization, resources, writing – review & editing. Alfonso Grassi, visualization, resources, writing – review & editing. Carmine Capacchione, conceptualization, supervision, writing – review & editing.

Conflicts of interest

There are no conflicts to declare.

Acknowledgements

Financial Support from Ministero dell'Università della Ricerca (MUR, Roma, PRIN 2017-CO₂ as only source of carbons for monomers and polymers: a step forwards circular economy-CO₂ only) and Università degli Studi di Salerno are gratefully acknowledged. Dr. Patrizia Iannece, Dr. Patrizia Oliva, Dr. Mariagrazia Napoli, and Dr. Ivano Immediata from Università degli Studi di Salerno for technical assistance are deeply acknowledged.

References

- 1 A. Chamas, H. Moon, J. Zheng, Y. Qiu, T. Tabassum, J. H. Jang, M. Abu-Omar, S. L. Scott and S. Suh, *ACS Sustainable Chem. Eng.*, 2020, **8**, 3494–3511.
- 2 R. Geyer, J. R. Jambeck and K. L. Law, *Sci. Adv.*, 2017, **3**, e1700782.
- 3 H. Nakajima, P. Dijkstra and K. Loos, *Polymers*, 2017, **9**, 523.
- 4 D. M. Mitrano and M. Wagner, *Nat. Rev. Mater.*, 2021, **7**, 71–73.
- 5 Q. Zhang, M. Song, Y. Xu, W. Wang, Z. Wang and L. Zhang, *Prog. Polym. Sci.*, 2021, **120**, 101430.
- 6 C. Vilela, A. F. Sousa, A. C. Fonseca, A. C. Serra, J. F. J. Coelho, C. S. R. Freire and A. J. D. Silvestre, *Polym. Chem.*, 2014, **5**, 3119–3141.
- 7 D. K. Schneiderman and M. A. Hillmyer, *Macromolecules*, 2016, **49**, 2419–2428.
- 8 K. M. Zia, A. Noreen, M. Zuber, S. Tabasum and M. Mujahid, *Int. J. Biol. Macromol.*, 2016, **82**, 1028–1040.
- 9 F. Siragusa, C. Detrembleur and B. Grignard, *Polym. Chem.*, 2023, **14**, 1164–1183.
- 10 G. A. Bhat, M. Luo and D. J. Darensbourg, *Green Chem.*, 2020, **22**, 7707–7724.
- 11 Y. Wang and D. J. Darensbourg, *Coord. Chem. Rev.*, 2018, **372**, 85–100.
- 12 C. M. Kozak, K. Ambrose and T. S. Anderson, *Coord. Chem. Rev.*, 2018, **376**, 565–587.
- 13 R. D. Rittinghaus and S. Herres-Pawlis, *Eur. J. Chem.*, 2023, **29**, e202202222.
- 14 S. Cui, J. Borgemenke, Z. Liu and Y. Li, *J. CO₂ Util.*, 2019, **34**, 40–52.
- 15 F. Della Monica and A. W. Kleij, *Polym. Chem.*, 2020, **11**, 5109–5127.
- 16 B. Grignard, S. Gennen, C. Jérôme, A. W. Kleij and C. Detrembleur, *Chem. Soc. Rev.*, 2019, **48**, 4466–4514.
- 17 C. A. L. Lidston, S. M. Severson, B. A. Abel and G. W. Coates, *ACS Catal.*, 2022, **12**, 11037–11070.
- 18 F. M. Haque, J. S. A. Ishibashi, C. A. L. Lidston, H. Shao, F. S. Bates, A. B. Chang, G. W. Coates, C. J. Cramer, P. J. Dauenhauer, W. R. Dichtel, C. J. Ellison, E. A. Gormong, L. S. Hamachi, T. R. Hoye, M. Jin, J. A. Kalow, H. J. Kim, G. Kumar, C. J. LaSalle, S. Liffland, B. M. Lipinski, Y. Pang, R. Parveen, X. Peng, Y. Popowski, E. A. Prebhalo, Y. Reddi, T. M. Reineke, D. T. Sheppard, J. L. Swartz, W. B. Tolman, B. Vlaisavljevich, J. Wissinger, S. Xu and M. A. Hillmyer, *Chem. Rev.*, 2022, **122**, 6322–6373.
- 19 X. Wang, Z. Huo, X. Xie, N. Shanaiah and R. Tong, *Chem. – Asian J.*, 2023, **18**, e202201147.
- 20 G. L. Gregory, G. S. Sulley, J. Kimpel, M. Lagodzińska, L. Häfele, L. P. Carrodegua and C. K. Williams, *Angew. Chem., Int. Ed.*, 2022, **134**, e202210748.
- 21 D. H. Lamparelli and C. Capacchione, *Catalysts*, 2021, **11**, 961.
- 22 C. Romain and C. K. Williams, *Angew. Chem., Int. Ed.*, 2014, **53**, 1607–1610.
- 23 M. W. Lehenmeier, S. Kissling, P. T. Altenbuchner, C. Bruckmeier, P. Deglmann, A.-K. Brym and B. Rieger, *Angew. Chem., Int. Ed.*, 2013, **52**, 9821–9826.
- 24 S. Kissling, P. T. Altenbuchner, M. W. Lehenmeier, E. Herdtweck, P. Deglmann, U. B. Seemann and B. Rieger, *Eur. J. Chem.*, 2015, **21**, 8148–8157.
- 25 S. Kissling, M. W. Lehenmeier, P. T. Altenbuchner, A. Kronast, M. Reiter, P. Deglmann, U. B. Seemann and B. Rieger, *Chem. Commun.*, 2015, **51**, 4579–4582.
- 26 S. Klaus, S. I. Vagin, M. W. Lehenmeier, P. Deglmann, A. K. Brym and B. Rieger, *Macromolecules*, 2011, **44**, 9508–9516.
- 27 Y. Liu, J.-Z. Guo, H.-W. Lu, H.-B. Wang and X.-B. Lu, *Macromolecules*, 2018, **51**, 771–778.



- 28 F. de la Cruz-Martínez, M. M. de Sarasa Buchaca, J. Martínez, J. Tejada, J. Fernández-Baeza, C. Alonso-Moreno, A. M. Rodríguez, J. A. Castro-Osma and A. Lara-Sánchez, *Inorg. Chem.*, 2020, **59**, 8412–8423.
- 29 A. Thevenon, J. A. Garden, A. J. P. White and C. K. Williams, *Inorg. Chem.*, 2015, **54**, 11906–11915.
- 30 G. Rosetto, A. C. Deacy and C. K. Williams, *Chem. Sci.*, 2021, **12**, 12315–12325.
- 31 A. J. Plajer and C. K. Williams, *Angew. Chem., Int. Ed.*, 2021, **60**, 13372–13379.
- 32 V. Paradiso, V. Capaccio, D. H. Lamparelli and C. Capacchione, *Coord. Chem. Rev.*, 2021, **429**, 213644.
- 33 A. Buonerba, A. De Nisi, A. Grassi, S. Milione, C. Capacchione, S. Vagin and B. Rieger, *Catal. Sci. Technol.*, 2015, **5**, 118–123.
- 34 A. Buonerba, F. Della Monica, A. De Nisi, E. Luciano, S. Milione, A. Grassi, C. Capacchione and B. Rieger, *Faraday Discuss.*, 2015, **183**, 83–95.
- 35 F. Della Monica, S. V. C. C. Vummaleti, A. Buonerba, A. D. Nisi, M. Monari, S. Milione, A. Grassi, L. Cavallo and C. Capacchione, *Adv. Synth. Catal.*, 2016, **358**, 3231–3243.
- 36 F. Della Monica, M. Leone, A. Buonerba, A. Grassi, S. Milione and C. Capacchione, *Mol. Catal.*, 2018, **460**, 46–52.
- 37 F. Della Monica, B. Maity, T. Pehl, A. Buonerba, A. De Nisi, M. Monari, A. Grassi, B. Rieger, L. Cavallo and C. Capacchione, *ACS Catal.*, 2018, **8**, 6882–6893.
- 38 F. Della Monica, A. Buonerba and C. Capacchione, *Adv. Synth. Catal.*, 2019, **361**, 265–282.
- 39 F. Della Monica, A. Buonerba, V. Paradiso, S. Milione, A. Grassi and C. Capacchione, *Adv. Synth. Catal.*, 2019, **361**, 283–288.
- 40 F. Niknam, V. Capaccio, M. Kleybolte, D. H. Lamparelli, M. Winnacker, G. Fiorani and C. Capacchione, *ChemPlusChem*, 2022, **87**, e202200038.
- 41 F. Della Monica, V. Paradiso, A. Grassi, S. Milione, L. Cavallo and C. Capacchione, *Chem. – Eur. J.*, 2020, **26**, 5347–5353.
- 42 I. Contento, D. H. Lamparelli, A. Buonerba, A. Grassi and C. Capacchione, *J. CO2 Util.*, 2022, **66**, 102276.
- 43 V. Paradiso, F. Della Monica, D. H. Lamparelli, S. D'Aniello, B. Rieger and C. Capacchione, *Catal. Sci. Technol.*, 2021, **11**, 4702–4707.
- 44 A. M. Hollas, J. W. Ziller and A. F. Heyduk, *Polyhedron*, 2018, **143**, 111–117.
- 45 M. Taherimehr and P. P. Pescarmona, *J. Appl. Polym. Sci.*, 2014, **131**, 41141.
- 46 R. Chiarcos, M. Laus, K. Sparnacci, R. Po, P. Biagini, I. Tritto, L. Boggioni and S. Losio, *Eur. Polym. J.*, 2023, **192**, 112058.
- 47 C. T. Cohen, T. Chu and G. W. Coates, *J. Am. Chem. Soc.*, 2005, **127**, 10869–10878.
- 48 G. Si, L. Zhang, B. Han, H. Zhang, X. Li and B. Liu, *RSC Adv.*, 2016, **6**, 22821–22826.
- 49 R. C. Jeske, J. M. Rowley and G. W. Coates, *Angew. Chem., Int. Ed.*, 2008, **47**, 6041–6044.
- 50 J. Y. Jeon, S. C. Eo, J. K. Varghese and B. Y. Lee, *Beilstein J. Org. Chem.*, 2014, **10**, 1787–1795.
- 51 S. Huijser, E. HosseiniNejad, R. Sablong, C. de Jong, C. E. Koning and R. Duchateau, *Macromolecules*, 2011, **44**, 1132–1139.
- 52 G. W. Coates and D. R. Moore, *Angew. Chem., Int. Ed.*, 2004, **43**, 6618–6639.
- 53 M. R. Kember, F. Jutz, A. Buchard, A. J. White and C. K. Williams, *J. Chem. Sci.*, 2012, **3**, 1245–1255.

